DOI 10.1002/pmic.200300456 *Proteomics* 2003, *3,* 1476–1485

**Raymonde Porchet[1]**
**Alphonse Probst[2]**
**Constantin Bouras[3]**
**Eduarda Dráberová[4]**
**Pavel Dráber[4]**
**Beat M. Riederer[1,5]**

[1]Institut de Biologie Cellulaire et de Morphologie, Lausanne, Switzerland
[2]Institute of Pathology, University Hospital Basel, Switzerland
[3]Department of Psychiatry, University of Geneva School of Medicine, Geneva, Switzerland
[4]Institute of Molecular Genetics, Academy of Sciences, Prague, Czech Republic
[5]Centre des Neurosciences Psychiatriques, Hôpital Psychiatrique, Prilly, Switzerland

# Analysis of gial acidic fibrillary protein in the human entorhinal cortex during aging and in Alzheimer's disease

Glial fibrillary acidic protein, GFAP, is a major intermediate filament protein of glial cells and major cytoskeletal structure in astrocytes. The entorhinal cortex has a key role in memory function and is one of the first brain areas to reveal hallmark structures of Alzheimer's disease and therefore provides an ideal tissue to investigate incipient neurodegenerative changes. Here we have analyzed age- and disease-related occurrence and composition of GFAP in the human entorhinal cortex by using one- and two-dimensional electrophoresis, Western blots and immunocytochemistry combined with confocal microscopy. A novel monoclonal antibody, GF-02, was characterized that mainly reacted with intact GFAP molecules and indicated that more acidic and soluble GFAP forms were also more susceptible to degradation. GFAP and vimentin increased with aging and in Alzheimer's disease (AD). Two-dimensional electrophoresis and Western blots revealed a complex GFAP pattern, both in aging and AD with different modification and degradation forms. Immunohistochemistry indicated that reactive astrocytes mainly accumulated in relation to neurofibrillary tangles and senile plaques in deeper entorhinal cortex layers. GFAP may be used as an additional but not exclusive diagnostic tool in the evaluation of neurodegenerative diseases because its levels change with age and respond to senile plaque and tangle formation.

**Keywords:** Astrocytes / Cytoskeleton / Tangles / Two-dimensional gel electrophoresis / Vimentin / Western blots PRO 0456

## 1 Introduction

Astrocytes have a variety of functions and form developmental scaffolds, provide boundaries and guidance for neuronal migration, and a structural, metabolic and trophic support to neurons [1]. Most importantly, they are closely linked to neuron energy metabolism and synaptic activity [2, 3]. Furthermore, any type of central nervous system injury may stimulate astrocytes to proliferate, to hypertrophy and to build glial filaments. Astrogliosis is also well known to occur in Alzheimer's disease (AD) [4–6]. AD is a dementing illness which clinically is characterized by intellectual decline and morphologically by senile plaques, dystrophic neurites and neurofibrillary tangles (NFT). Presently, the pathological diagnosis of AD is mainly based on the distribution and density of NFT [7], and both, senile plaques and NFT, have been shown to be correlated with the severity of dementia in AD [8–10]. Braak and colleagues [7] also have identified the entorhinal cortex as a pivotal area among affected brain regions in AD, since the very first neurofibrillary lesions are detectable here and together with the temporobasal isocortex belong to regions where the first senile plaques are formed [10]. The pathophysiological mechanisms responsible for plaque formation and progression are emerging. Glial cells, and among them astrocytes and microglia are likely to play a key role in the formation of senile plaques [11]. Astrocytes were found to be associated with many but not all senile plaques [12]. In addition to the classical lesions, astrocytosis is a well known feature of AD and the association of astrocytes with plaques is well established [13, 14]. Astrocytes colocalize with a dense amyloid core and an attendant microglial reaction *via* interleukin (IL)1β hypertrophy of astrocytes [12]. Confocal microscopy and 3-D reconstruction have demonstrated that astrocytes surround plaques and many astrocytic processes penetrate into the plaque core [15]. Nevertheless, such astrocytic reactions may occur during the normal aging process, independently of the formation of senile plaques.

The GFAP is the building block of glial intermediate filaments and is the major cytoskeletal structure in astrocytes [16]. Human GFAP is composed of 432 amino acids

**Correspondence:** Dr. B. M. Riederer, Institut de Biologie Cellulaire et de Morphologie, Rue du Bugnon 9, 1005 Lausanne, Switzerland
**E-mail:** beatmichel.riederer@ibcm.unil.ch
**Fax:** +41-21-692-5105

**Abbreviations: AD**, Alzheimer's disease; **APP**, amyeloid precursor protein; **GFAP**, glial acidic fibrillary protein; **NFT** neurofibrillary tangle; **PHF**, paired helical filament; **pmd**, *post mortem* delay

with an apparent mass of 51 kDa and a calculated mass of 49 880 Da, and p*I* of pH 5.4. The chromosome map location of the GFAP gene is 17q21. GFAP is characterized by coiled-coil domains, which are essential for filament formation. It is used also as a marker for astrocytes. Another marker for astrocytes, but not exclusively, is vimentin, but it localizes more in immature astrocytes, while GFAP is found rather in mature astrocytes, during aging and in reactive astrocytes [17, 18]. Furthermore, the molecular structure of GFAP is modified during development and aging and responds dynamically to neurodegenerative lesions [19]. Brain lesions induce local activation of astrocytes and microglia events that are mediated by cytokines and growth factors such as IL-1, IL-6, TGF-$\alpha$, TGF-1 and bFGF, [17 for review]. Microglia, IL-1 as well as apolipoprotein E and $\beta$amyleoid precursor protein (APP) may contribute towards plaque formation [11]. Furthermore, the dynamic properties of GFAP may depend on post-translational modifications such as phosphorylation of several sites in the GFAP head domain [20].

Many cytoskeletal proteins undergo age- and disease-related post-translational changes [21] and tau proteins have received much attention because of their particular or abnormal hyperphosphorylation and their role in the formation of paired helical filaments (PHF) which are considered among hallmark structures of Alzheimer's disease. Two-dimensional electrophoresis and monoclonal antibodies are valuable tools for the identification of general protein changes and to identify specific proteins and their modifications respectively. Here we have investigated protein changes in autopsy tissue from the entorhinal cortex of control and AD subjects by using the powerful tool of 2-DE analysis and combined it with immunoblotting, immunocytochemical and confocal microscopical analysis. We focused mainly on GFAP and its role during aging and Alzheimer's disease and compared it to PHF and plaque distribution. We have also characterized a novel antibody for human GFAP, which reacts with intact but not with *N*-terminally degraded GFAP molecules.

## 2 Materials and methods

### 2.1 Tissues

After autopsy, parts of the human entorhinal cortex were either immediately frozen at $-80$°C for subsequent biochemical analysis or tissue samples were fixed with 4% paraformaldehyde for 48 h, rinsed with PBS, and kept at 4°C until immunohistochemical procedures. Autopsy human brain tissues were obtained from six controls and five cases with confirmed Alzheimer's disease:

(1) from a 52 year old female without cognitive decline. She was suffering from urinary bladder carcinoma and died due to heart failure. The brain was obtained 4 h after death.
(2) from a 56 year old male who died due to heart failure after suffering from buccal and pulmonary carcinoma. No dementia was recorded. Brain was obtained 10 h after death.
(3) from a 59 year old male with hypopharynx and esophagus cancer, without neurological history. Death was due to heart failure. The brain was obtained 10 h after death.
(4) from a 62 year old female, with arterial hypertension but without neurological history. Death was due to cerebral hemorrhage. Brain was obtained 7 h after death.
(5) from a 78 year old, intellectually preserved male, with diabetes mellitus, arterial hypertension and colon carcinoma. Brain was obtained 11 h after death.
(6) from a 79 year old male without intellectual decline. Death was due to cholecystitis and septicemia. Brain was obtained 5 h after death
(7) from a 79 year old demented male patient with AD on *postmortem* examination (Braak stage V). Death was due to pulmonary embolism. Brain was obtained 10 h after death.
(8) from a 84 year old demented female patient, with AD (Braak stage VI), generalized arteriosclerosis and heart failure due to acute pyelonephritis. Brain was obtained 13 h after death.
(9) from a 90 year old demented female patient AD (Braak stage VI) and generalized arteriosclerosis. Death was due to bronchpneumonia. Brain was obtained 2.5 h after death.
(10) from a 94 year old demented female patient with AD (Braak stage III) and diffuse cortical brain atrophy. Death was due to pulmorary embolism. Brain tissues were collected 5 h after death.
(11) from a 94 year old female patient with Alzheimer changes in the brain corresponding to a Braak stage III. Death was due to heart failure. Brain was obtained 8 h after death.

For a variety of measurements, additional brain tissue samples (temporal lobe) were collected from a 68 year old male with mild AD (Braak stage III; *post mortem* delay (pmd) 5 h), for initial antibody screening. For immunoprecipitation, samples of the frontal cortex from a 88 year old female with AD (Braak stage IV) (pmd 3 h) was used. In addition to above-mentioned samples, entorhinal cortex tissue of a 86 year old female, 6 h pmd without neuropathological alterations and of a 93 year old female, 8 h pmd with severe AD were used for proteomic analysis.

### 2.2 Antibodies

Several well characterized antibodies were used: rabbit polyclonal antibody GFAP (1:2,000 dilution) from DAKO (Zug, Switzerland) mouse mAb GF-01 (IgG1) against GFAP was used at 1:1000 dilution [22] and mouse mAb V9 (immunoglobulin (Ig)G1) against vimentin from Boehringer Mannheim, (Mannheim, Germany) was used at a 1:50 dilution. AD2 used at 1:10 000 dilution is a murine mAb that reacts with the upstream flanking region of the microtubule-binding domain when Ser396 and Ser404 are phosphorylated. These are phosphorylation sites which remain stable in neurofibrillary lesions even in autopsy tissues thus making AD2 useful for their detection [23]. The mouse monoclonal AT8 antibody at a 1:1000 dilution recognizes human tau isoforms when phosphorylated at serine residue 202 and threonine 205 of the largest human tau form [24]. The polyclonal antibody against the βA peptide 1–42 was obtained from DAKO and was used at a 1:50 dilution. The hybridoma cell line producing novel anti-GFAP antibody GF-02 was obtained after immunization of Balb/c mouse with a pellet of pig brain cold-stable proteins after depolymerization of microtubules. This material was used for initial screening. The immunization protocol, the technique for the fusion of spleen cells with mouse myeloma cells Sp2/0, the screening, cloning and subcloning methods and ascites production have been described previously [25, 26]. Immunoglobulin subclass was determined using a mouse mAb isotyping kit Isostrip (Roche, Mannheim, Germany).

### 2.3 Immunoprecipitation

For immunoprecipitation, 260 mg human frontal cortex from a 88 year old female with short pmd was homogenized in 500 μL extraction buffer (20 mM Tris, 0.8 M NaCl, 0.2 mM DTT, 5 mM $MgCl_2$, 1 mM EGTA, 0.5% Triton X-100, pH 8.3), in the presence of 10 μg/mL leupeptin, antipain and E64 (Sigma, Buchs, Switzerland). Nonspecific protein binding was absorbed by an incubation with 200 μL pansorbin (Calbiochem-Novabiochem, La Jolla, CA, USA). One hundred and fifty μL of supernatant was incubated with 15 μL of GFAP antibody for 2 h followed by 60 μL pansorbin for another hour. The antigen-antibody *Staphylococcus aureus* complex was sedimented (11 000 × *g*, 2 min) and washed several times with extraction buffer, dissolved in 90 μL SDS sample buffer and separated on SDS-PAGE. Proteins were either stained with Coomassie Blue or transferred to nitrocellulose filters and immunostained with antibodies.

### 2.4 Electrophoresis and immunobloting

Defined amounts of proteins were separated by 3.6–15% SDS-PAGE and either stained with Coomassie Brilliant Blue or electrophoretically transferred to nitrocellulose filters and immunostained with monoclonal and polyclonal antibodies. Proteins were either detected with antibodies and peroxidase-conjugated secondary antibodies followed by incubation with 4-chloro-1-naphthol [27] or by a chemiluminescent reaction. In short, membranes were washed in PBS (5 mM $Na_2$ $HPO_4$ + 155 mM NaCl pH 7.4) and nonspecific binding sites were blocked by incubation in 5% dried milk in PBS + 0.15% Tween 20 for at least 30 min. After rinsing with PBS filters were incubated with primary antibodies in 2.5% dried milk in PBS and 0.15% Tween for 60 min at room temperature. Antibodies were used at dilutions: 1:1000 (GF-01), 1:5000 (GF-02), 1:20 000 (rabbit anti-GFAP) or 1:25 (V9, antivimentin). After several rinsing steps in PBS, membranes were incubated for 60 min at room temperature with peroxidase-conjugated rabbit-antimouse Ig or goat-antirabbit Ig (Amersham Biosciences, Dübendorf, Switzerland) diluted 1:2000 in 2.5% dried milk, PBS and Tween. Filters were rinsed several times with PBS. The membranes were incubated for exactly 1 min to a mixture of one part detection solution 1 and one part detection solution 2 (ECL; Amersham Biosciences) as described by the manufacturer. Excess solution was drained and filters were wrapped in SaranWrap and quickly exposed to Kodak Biomax MR autoradiography film for several seconds or minutes. The intensity of immunostaining was quantified by a densitometry software (1D Main; American Applied Biotechnology, Fullerton, CA, USA) by measuring the spot intensity.

### 2.5 2-DE

Brain tissue was homogenized with 1:10 w/v denaturation buffer (5 M urea + 2 M thiourea 35 mM Tris + 4% CHAPS + 1% dithioerythritol (DTE)) followed by protein determination (Bio-Rad, Reinach, Switzerland). For first dimension at separation, Immobiline DryStrips pH 3.5–10, 18 cm long (Amersham Biosciences) were rehydrated with 200 μg of proteins adjusted overnight in 1 mL with rehydration buffer (8 M urea + 2% CHAPS + 9.72 mM DTE + 2% Pharmalyte 3–10 + 1% bromphenol blue). The strips were then covered with mineral oil and the proteins were separated for 98 000 Vh at 15°C. For the second dimension, strips were first incubated in equilibration buffer (6 M urea + 0.5 M Tris-HCl pH 6.8 + 2% SDS + 30% glycerol v/v) + 2% DTE + 0.5% bromphenol blue for 15 min and second in equilibration buffer + 2.5% iodoacetamide + 0.5%o bromphenol blue for 15 min. The proteins were

then separated on a 9–16% acrylamide gel prepared from a stock solution: 30% acrylamide + 0.8% piperazine diacrylamide + 5% sodiumthiosulfate + 1.5 M Tris-HCl, pH 8.8). Migration was performed with 40 mA/gel in Laemmli buffer (0.05 M Tris + 0.39 M glycine + 0.2% SDS) at 15°C for 5 h. Proteins were visualized by silver staining [28].

### 2.6 Immunohistochemistry

For immunohistochemistry, entorhinal cortex tissue was immersed in 4% paraformaldehyde in PBS for 48 h. Tissue was stored in PBS at 4°C, and incubated for 24 h in 30% sucrose and PBS at 4°C, prior to cutting. Sections of 50 μm thickness were cut with a Microm HM400 (Heidelberg, Germany) congelation microtome. Some sections were also stored in series in a freeze protection solution (150 g sucrose, 300 mL ethylene glycol, 500 mL 50 mM PBS pH 7.4, 200 mg Na-azide). Sections were kept at −20°C until use. Free-floating sections were rinsed with TBS, Tris 0.5 M + NaCl 121 mM, pH 7.2) at 4°C, all subsequent steps were performed at room temperature. Sections were incubated for 30 min in 3% fetal calf serum (FCS) in TBS to block nonspecific antibody binding sites, followed by an incubation overnight with rabbit anti-GFAP at 1:200 dilution and AD2 at 1:10 000 (0.26 μg/mL) in TBS supplemented with 1% FCS. The sections were rinsed several times with TBS and incubated for at least 2 h with 1:1000 diluted secondary antibodies Oregon green conjugated goat antimouse Ig and Texas red conjugated goat antirabbit (Molecular Probes, Leiden, The Netherlands). Sections were mounted on glass slides and covered with semisolid mounting fluid [29]. These sections were examined with a Leica confocal microscope (Leica TCS NT, Heidelberg, Germany), equipped with an argon-krypton laser set at 568 nm excitation. Picture size was between 284 kb to 1 Mb. For each series a stack of optical sections at different planes of focus was collected. Care was taken to use the full dynamic range of the photomultipliers by using a special look-up table (glow-over-glowunder, Leica). Digitized images were processed with image-editing software (Adobe Photoshop, Mountain View, CA, USA).

For Fig. 4, deparaffinized sections were treated with 0.3% $H_2O_2$ to block the endogenous peroxidase activity. Sections were incubated for 30 min at room temperature with normal goat serum and normal horse serum to block nonspecific sites before application of primary antibodies, monoclonal AT8 and polyclonal βA antibody, overnight at 4°C. Bound antibodies were visualized by using the avidin-biotin peroxidase method (Elite standard kit SK6100; Vector, Geneva, Switzerland). The peroxidase activity was revealed with a substrate solution containing 1% diamidobenzidine (DAB) and 3% $H_2O_2$. All sections were counterstained with hematoxylin. For GFAP, sections were processed in a Ventana Nexes (Strasbourg, France) automated slide stainer and using a related Ventana DAB detection kit.

## 3 Results

For the identification of GFAP and for the characterization of mAb GF-02 (IgM), a polyclonal antibody was used to immunoprecipitated GFAP from human brain tissue. Original homogenate and several steps in the precipitation process were separated by SDS-PAGE (Fig. 1). Coomassie blue staining demonstrates a protein of the $M_r$ of GFAP in immunoprecipitated sample (Fig. 1A, lane 5). Immunoblots with the GFAP immunoprecipitation experiment were stained with mAbs GF-01 (Fig. 1B) and GF-02 (Fig. 1C) or with the polyclonal anti-GFAP antibody (Fig. 1D). All antibodies identified immunoprecipitated GFAP in lane 5. The novel antibody GF-02 detected exclusively the intact GFAP, while GF-01 and the polyclonal antibody detected also degradation products of GFAP. Given that GFAP is mainly degraded at the *N*-terminal end [30] it seems likely that GF-02 is directed against the *N*-terminal site of GFAP.

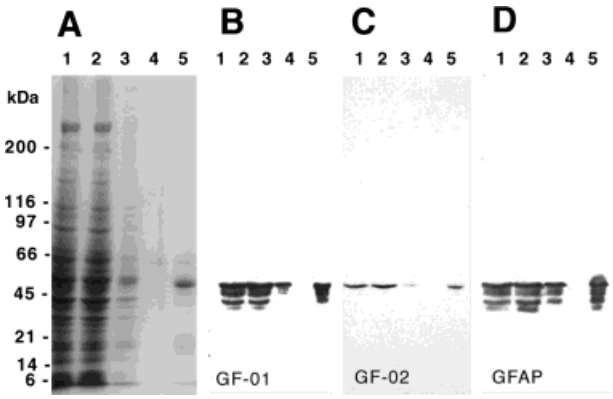


**Figure 1.** Immunoprecipitation of GFAP and specificity of GF-02 antibody for intact GFAP. Frontal cortex tissue (88 year old female, 3 h pmd, with presence of senile plaques) was used to immunoprecipitate human GFAP with a polyclonal antibody against GFAP and pansorbin. Proteins were separated by 3.6–15% gradient SDS-PAGE and stained with Coomassie blue (panel A). After electrophoretical transfer, nitrocellulose filters were used to stain blots with antibodies clone GF-01 (panel B), clone GF-02 (panel C) and polyclonal anti-GFAP (panel D). Protein samples are: in lane 1, brain homogenate before incubation; lane 2, brain homogenate after incubation with antibody and pansorbin; lane 3, prewash of brain homogenate with pansorbin only; in lane 4, pansorbin in PBS; and in lane 5, immunoprecipitated GFAP. The molecular weight is indicated on the left.

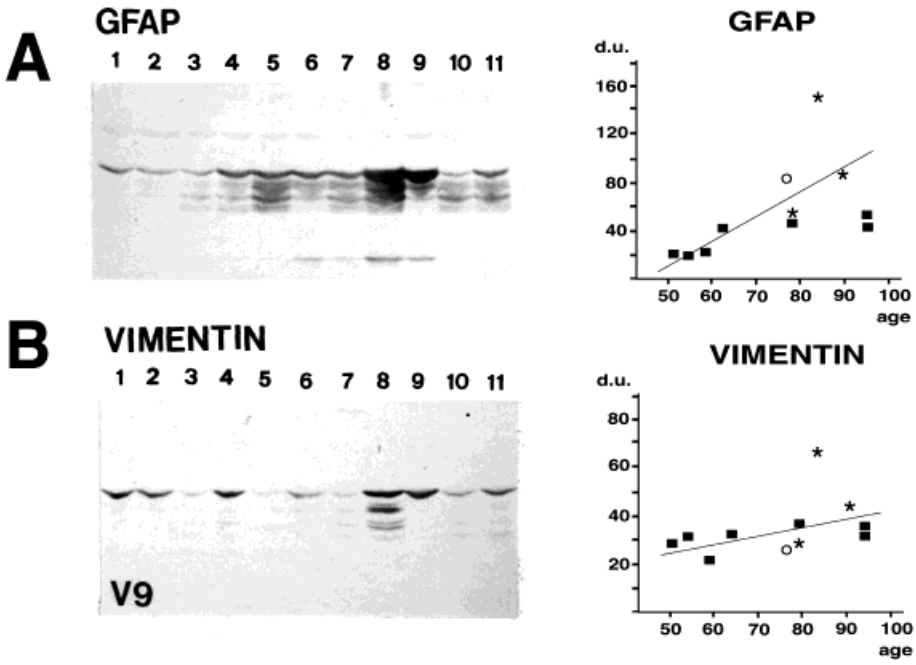


**Figure 2.** Western blots of entorhinal cortex tissues from 11 human subjects aged 52 to 94 years. The sequence of samples (total protein) corresponds to the numbering of cases in methods, Age/Sex/pmd (1: 52F4, 2: 56M10, 3: 59M10, 4: 62F7, 5: 78M11, 6: 79M5, 7: 79M10, 8: 84F13, 9: 90F2.5, 10: 94F5, 11: 94F8). Protein samples were separated by a 3.6–15% gradient SDS-PAGE and transferred to nitrocellulose. Blots were exposed to polyclonal anti-GFAP antibody (A) and anti-vimentin antibody V9 (B). Sample 8 with largest amounts of GFAP and vimentin degradation products is also the sample with longest *post mortem* delay and severest form of AD (Braak stage VI). In the graphs next to the blots the densitometrical values of GFAP and vimentin immunoreactivity were plotted against age (in years). Severest AD cases are indicated with an asterisk, while the sample with isolated senile plaques is indicated with a circle; all other cases are indicated with a square. Linear regression coefficient was r = 0.53 for GFAP and r = 0.37 for vimentin. d.u. represents densitometrical units ($\times$ 1000). Plotting the densitometrical values against the pmd does not indicate an increase of degradation with aging (not shown).

Eleven subjects were compared for the presence of GFAP and vimentin by Western blots. The samples are aligned from left to right by increasing age from 52 to 94 y. There was a trend towards increased GFAP immunoreactivity in older subjects, with more degradation products in ages above 78 y (Fig. 2A). Vimentin, another element found in astrocytes, was found in all samples, but its quantity was not proportional to that of GFAP. Samples 8 and 9 have a high GFAP and vimentin content, but with sample 8 having more degradation products of GFAP and vimentin than sample 9. Both samples are from subjects with AD (Braak stage VI), but with a considerable difference in *post mortem* delay. Case 8 has a delay of 13 h between death and autopsy, while for case 9 tissue samples were processed within 2.5 h after death. This suggests that a long *post mortem* delay may contribute to GFAP degradation in some cases. These Western blots were analyzed for staining intensity by densitometry and values were aligned in relation to the age of the subjects. GFAP and vimentin immunoreactivity were found to increase with age. However, the regression coefficients r = 0.53 for GFAP and r = 0.37 for vimentin suggest rather a trend than a strong correlation.

Two-dimensional separation of entorhinal cortex tissue by high resolution 2-DE followed by silver staining showed a two- to three-fold increase of GFAP and its degradation products in samples from AD subjects (square in Fig. 3B), while control samples had less GFAP degradation products and intact GFAP (Fig. 3A). For a better discrimination of the differences the squares were magnified (panel C and D). In parallel, several 2-DE gels were also transferred to nitrocellulose and immunostained with GFAP antibodies. Western blots stained with the polyclonal GFAP antibody demonstrated a similar GFAP pattern between younger and older subjects without neuropathological diseases (Fig. 3E and F). The intact GFAP top band, revealed at least 12 different spots. Smaller forms are found mainly in the more acidic range to the left and with smallest forms becoming more acidic. Given the differences in GFAP content, immunoreactivity was developed for a similar staining intensity. Some younger subjects also had lesser GFAP degradation. Although the GFAP levels were sometimes higher in AD, the repartition of intact and degraded GFAP was different (Fig. 3G). Less acidic forms of intact GFAP were detectable while smaller and more acidic forms were increased, suggesting

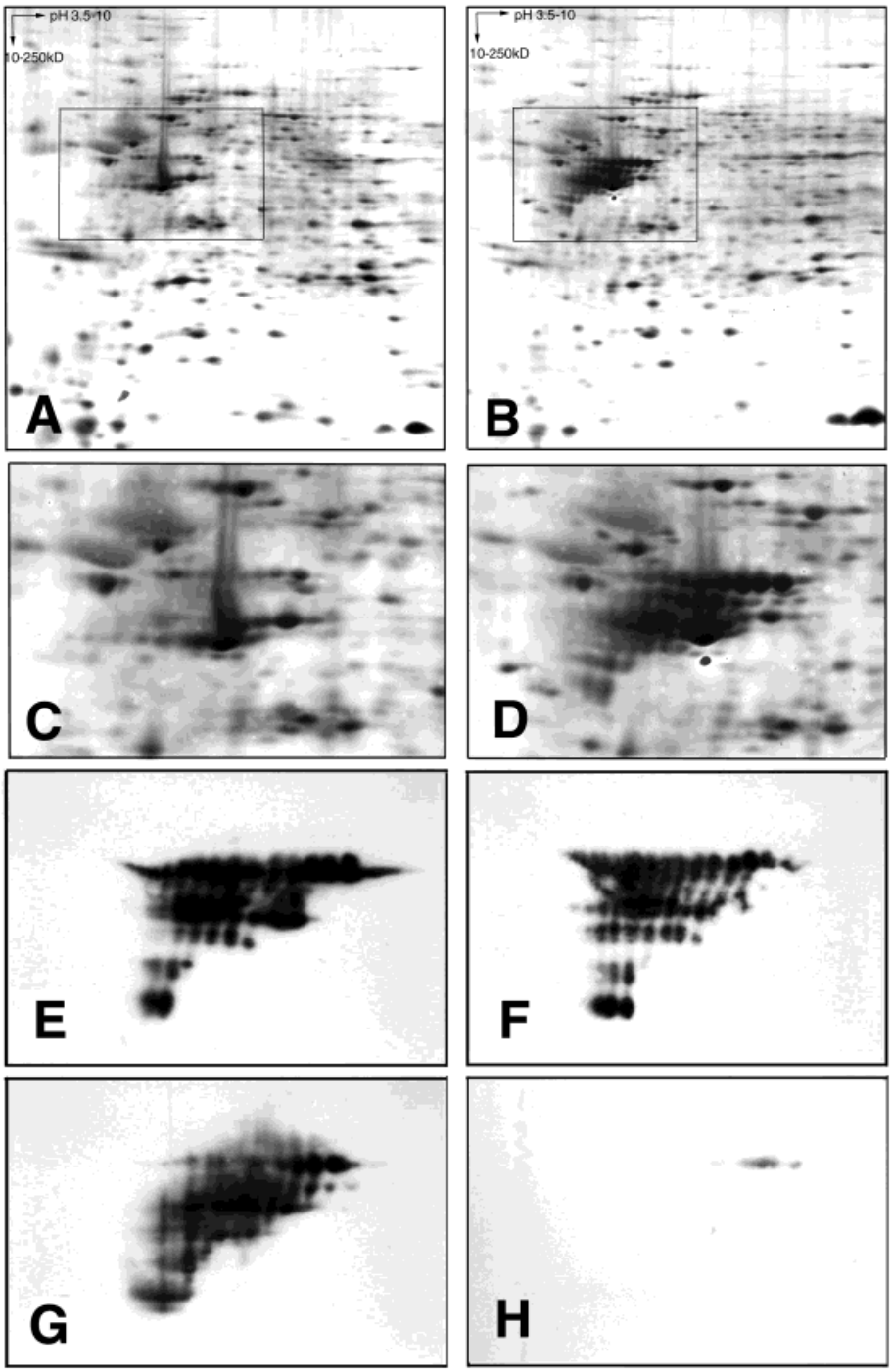


**Figure 3.** Representative silver stained gels and GFAP immunoblots of 2-DE separations of human entorhinal cortex tissue are shown. Protein separation within a focusing range of pH 4–8 is shown from left to right and a mass from 250 kDa to 10 kDa from top to bottom. A and C: 56 year old male, 10 h pmd, no neuropathological alterations; B and D: 84 year old female, 13 h pmd with severest form of AD. The location of GFAP is indicated by rectangles in A and B. These rectangles are also shown at higher magnification in C and D. The same areas were also transferred to nitrocellulose filters and immunostained for GFAP. For Western blots of 2-DE gels stained with anti-GFAP (panels E-G) and GF-02 (panel H), the following tissues were used E: 52 year old female, 4 h pmd, without neuropathological signs; F: 86 year old female, 6 h pmd without neuropathological alterations; G and H: 93 year old female, 8 h pmd and severe AD. Note that the GF-02 antibody in panel H detects exclusively more basic and intact GFAP.

increased degradation. The GF-02 staining of the same blot (Fig. 3H) was weak, and only the basic and uncleaved GFAP forms were identified.

In Fig. 4 the relationship of astrocytes, NFT and plaques in young and older control subjects and in AD are shown. GFAP immunostaining revealed fibrous astrocytes almost confined to the first (molecular) cortical layer (Fig. 4A) in the young control subject. Some reactive astrocytes are encountered in layer II (stellate cell layer) of the entorhinal cortex in the older control subject (Fig. 4B). In a patient with AD, GFAP positive astrocytes were found in layer II and deeper layers III and IV, in relation to βAPP-positive deposits and senile plaques (Fig. C and E). No AT8-positive NFT or βAPP positive deposits were found in young control subjects (D and G); numerous AT8-positive lesions

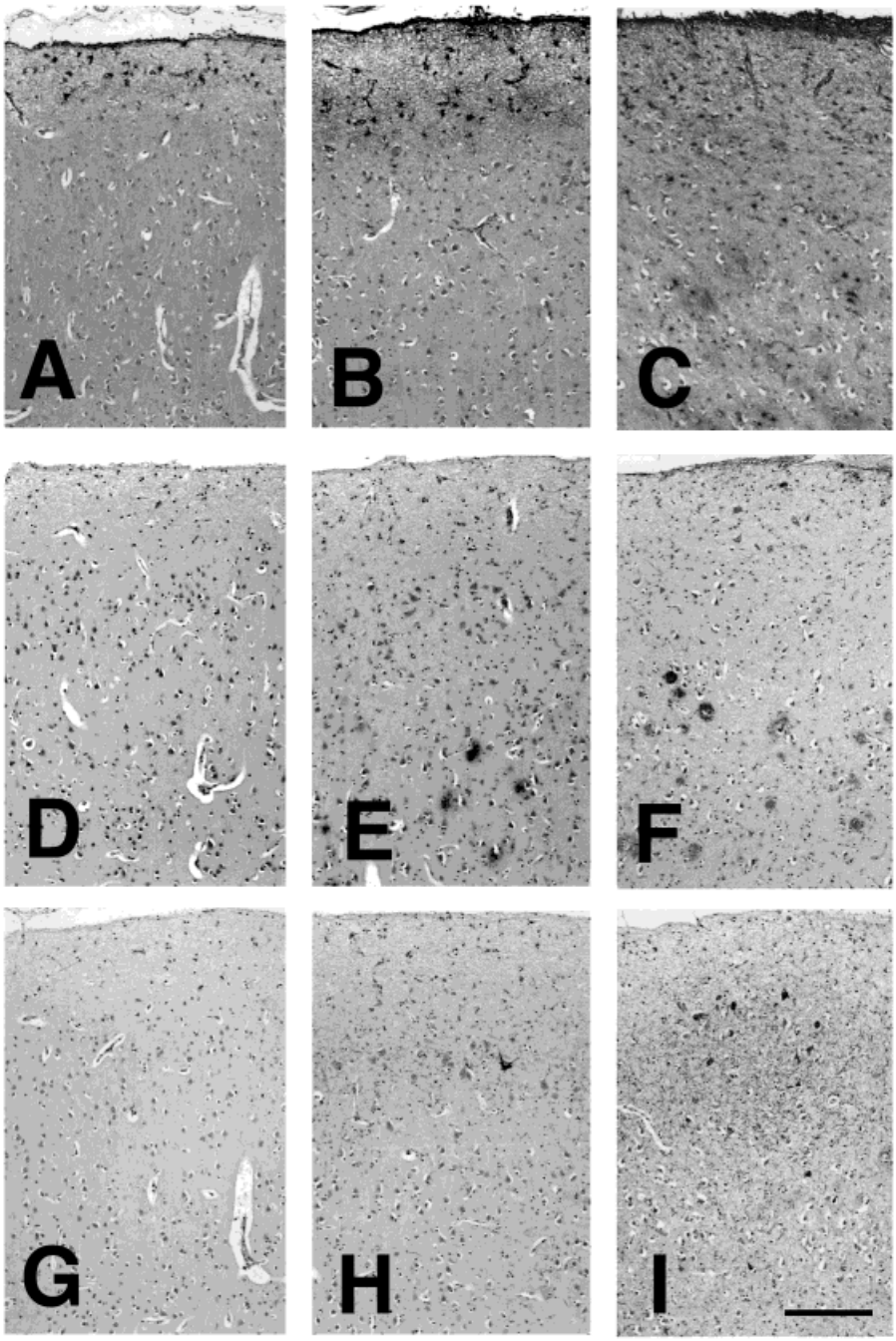


**Figure 4.** The panel shows a comparison of the extension and intensity of astrocytic gliosis, the number of senile plaques and the density of AT8-immunoreactive structures in the entorhinal cortex of three patients: a 52 year old female patient without brain disease (pmd 4 h) panels A, D and G; a 79 year old nondemented male patient (pmd 5 h) panels B, E and H; a 79 year old demented female patient with histologically verified Alzheimer's disease (pmd 10 h) panels C, F and I. Panels A-C represent GFAP-positive astrocyte distribution, panels D-F show the βA peptide and plaque distribution, while panels G-I show the AT8 positive neurons with PHF and thread-like fibers. Magnification bar = 200 μm.

were seen in layers II and III in an old nondemented patient (Fig. 4E and H). In a patient with AD (Fig. 4F and I) senile plaques, tangles and threads were numerous in layer II and deeper entorhinal cortex layers as well.

Confocal images of different areas of entorhinal cortex, double-labeled for GFAP in red and phosphorylated tau in green, document the relationship of astrocytes and neuritic elements in plaques (Fig. 5A), as well as the relationship of astrocytes and neurons with tangles (Fig. 5B). The tau antibody is directed against a tau form and modification that occurs in neurodegeneration. Therefore, Fig. 5A demonstrates in a spectacular way how astrocytes localize in layer II of the entorhinal cortex where an increased number of neurons was found, with a random distribution of PHF positive neurons and astrocytes

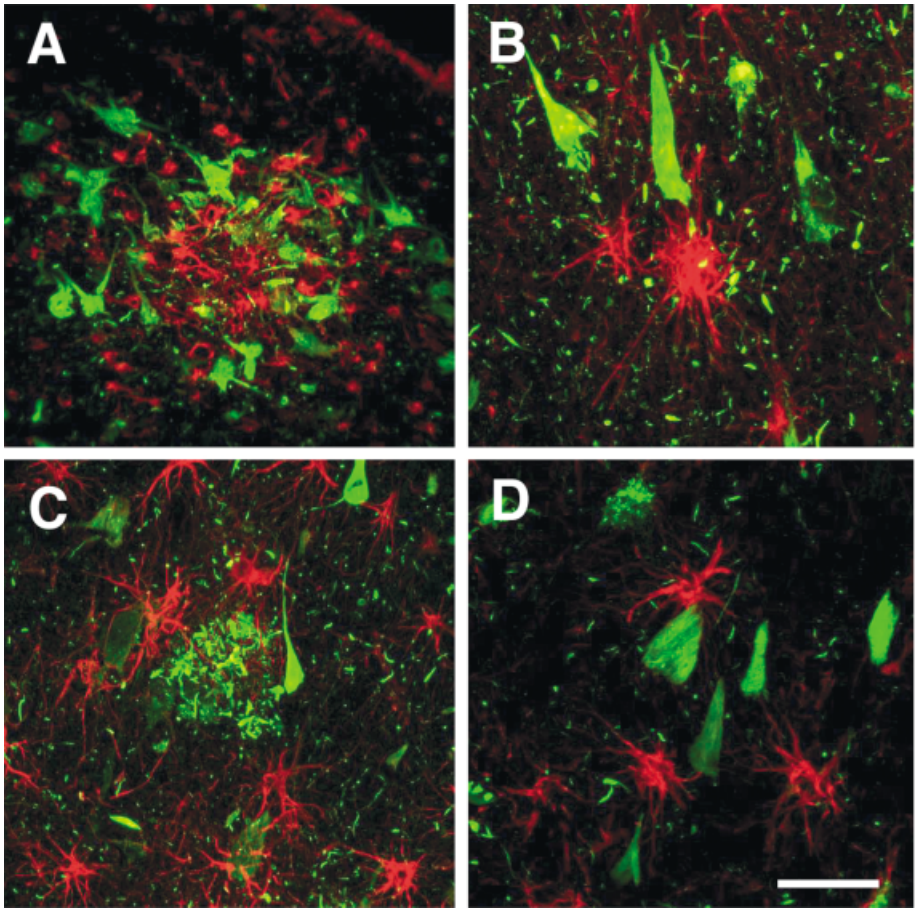


**Figure 5.** Confocal micrographs, showing double-labeling with polyclonal anti-GFAP antibody (red) and monoclonal anti-tau antibodyAD2 (green) in entorhinal cortex of a 84 year old female, 13 h pmd, with severe AD. In panel A, a cluster of tau-positive neurons of layer II (in green) is intermixed with reactive astrocytes (in red). Panels B and D show neurons with NFTs (in green) and astrocytes (red) in their vicinity. In panel C, many astrocytes (in red) gather around senile plaques and tau positive deposits (in green). Bar = 20 μm.

(Fig. 5B and D). Many more astrocytes were also localized in lower cortical layers near tau-positive senile plaques (Fig. 5C).

## 4 Discussion

In this report we have characterized a novel antibody for GFAP, GF-02. The antibody must be directed against the *N*-terminal part of GFAP because it reacts mainly with the intact molecule. Fujita and colleagues [30] have shown that during motor neuron degeneration of a mutant mouse GFAP is degraded by cleavage of 29 and 56 *N*-terminal sequences, resulting in a similar pattern as we have observed in 2-DE gels, with more acidic degradation products. The susceptibility of GFAP to degradation with increasing *post mortem* delay is debated [30, 31]. In our study, the case with the longest pmd also showed highest GFAP degradation and was from a subject with severe AD. As a comparison, minor GFAP degradation was observed in a case with severe AD and very short pmd. This suggests that extended pmd may add to GFAP degradation. The presence of some degradation products with GF-02 may also indicate that cleavage at the *C*-terminal end is possible but less frequent, and only found in cases with increased GFAP degradation products. In rhesus monkey, astrocytic hypertrophy and altered GFAP degradation with age has been described in subcortical white matter [32], and in primary cultures of rat astrocytes a calcium-dependent proteolysis of vimentin and GFAP was identified [33]. Our 2-DE gel analysis of severe AD cases confirms that more acidic forms of GFAP are more easily degraded, possibly by calcium-dependent proteases such as calpain. GFAP is subject to post-translational modifications, mainly phosphorylation which is essential in filament formation [20]. In 2-DE gels a variety of GFAP spots reflect different degrees of modification responsible for changes in the protein migration during electrofocusing. The *N*-terminal part or head domain of GFAP contains five phosphorylation sites [20], the *N*-terminal end of more acidic GFAP forms seem also more vulnerable to cleavage by calpain [30]. Phosphorylation may play a role in the assembly and filament formation, and such modifications are key elements in astrocytic plasticity.

GFAP concentrations in cerebrospinal fluid correlate with age and several forms of dementia except frontal lobe dementia [34]. In another 2-DE study, sera from 46 patients with AD and vascular dementia were screened for auto-antibodies against GFAP [35]. Several patients had developed auto-antibodies to the more basic components of GFAP. GFAP forms with higher p*I* are more insoluble and less degraded, as a result auto-antibodies are likely to be found against the more degradation susceptible and acidic forms. Therefore, we can conclude that the novel antibody, GF-02, reacts with intact, more basic and insoluble GFAP.

We have shown that GFAP concentration and its degradation are increased in many entorhinal cortex autopsy tissues obtained from elderly and AD subjects. This is in agreement with many reports on GFAP in human and animal brain [4–6, 32, 36]. Human GFAP is susceptible to several post-translational modifications and our 2-DE results demonstrate that mainly acidic forms are degraded in AD, as described for rat GFAP [33]. GFAP, as typical astrocytic protein, provides an additional marker to indicate neurodegenerative changes. An increase of GFAP is however not exclusive for neurodegeneration. In an experimental model, a decrease of MAP2 and neurofilament proteins and an up-regulation of GFAP several hours after the injury were observed [37, 38]. An increase of GFAP, as in astrogliosis, is defined by an increased number of astrocytes and hypertrophy of these cells and also can be observed in many other processes like inflammation of the CNS or vascular injury. Nor does an increase of GFAP distinguish between neurodegenerative diseases or vascular insults [39].

In AD, astrocytosis has been mainly described in relation to senile plaques [13, 14, 40]. Characteristic structures as well as putative molecular events responsible for plaque formation have been reviewed recently [11, 12]. Here we have identified the location of plaques by the presence of GFAP-stained hypertrophic astrocytes around an amyloid center, and by using a tau antibody that reacts with tau in PHF, with threads and neurites, constitutive elements of senile plaques. Astrocytes cluster around plaques in deeper layers of AD and were also found near PHF positive neurons, while in older controls astrocytes are limited to the top layer of the entorhinal cortex. This suggests a close relationship between astrocytes and dying neurons in AD. Layer II of the entorhinal cortex seems especially vulnerable because many astrocytes infiltrated this layer, which is characterized by many AD-tau positive neurons. Increase in GFAP is related to an increase of fibrous or hypertrophic astrocytes, which are found often in the vicinity of senile plaques [4–6, 36]. Our double-labeling experiment with antibodies against phosphorylated tau and GFAP suggests that several tau-positive senile plaques and clusters of PHF positive neurons may attract reactive astrocytes. Plaque-associated dystrophic neurites are a common feature in AD brains, and may contain GFAP and tau positive fibers. Dystrophic neurites can develop retrogradely from focal plaque damage to induce somatic and dendritic degeneration and potentially contribute to NFT formation [41].

Vimentin is known to be expressed in growing astrocytes and to be an element of immature intermediate filaments [17, 18]. In our samples vimentin values were variable and were not proportional to those of GFAP. This difference could be due to differences in the metabolic pathway and degradation [33]. Furthermore, vimentin is not exclusive to astrocytes and is also found in endothelial cells and microglia and therefore does not account exclusively for astrocytic changes.

## 5 Concluding remarks

In conclusion, GFAP proteomics may provide an additional tool to investigate molecular changes in AD, but given the role of astrocytes after any CNS insult GFAP values point to an increase of reactive astrocytes and astrogliosis and are not restricted to AD. Astrocytes are involved in many events and one of their roles may be to help neurons to survive neurodegeneration. GFAP is subject to degradation and its acidic forms seem more easily degraded in AD while more basic and insoluble GFAP isoforms typically detected by antibody GF-02, seem better able to resist the process of degradation.

*This work was supported by the Swiss National Science Foundation grants 31-53725.98 and 31-067201.01, by the Sandoz Foundation for Gerontological Research, and by the A. R. and J. Leenaards Foundation, and by the AETAS Foundation for Research on aging, and grant A 5052004 from Grant Agency of the Czech Academy of Sciences and LN00A026 from the Ministry of Education of the Czech Republic.*

Received December 4, 2002

## 6 References

[1] Kettenman, H., Ransom, B. R., *Neuroglia*, Oxford University Press, New York 1995.

[2] Magistretti, P. J., Pellerin, L., Rothman, D. L., Shulman, R. G., *Science* 1999, *283*, 496–497.

[3] Bezzi, P., Voltera, A., *Curr. Opin. Neurobiol.* 2001, *11*, 387–394.

[4] Mancardi, G. L., Liwnicz, B. H., Mandybur, T. I., *Acta Neuropathol.* 1983, *61*, 76–80.

[5] Beach, T. G., Walker, R., McGeer, E. G., *Glia* 1989, *2*, 420–436.
[6] Mandybur, T. I., Chiurazzi, C. C., *Neurology* 1990, *40*, 635–639.
[7] Braak, H., Braak, E., Bohl, J., *Eur. Neurol.* 1993, *33*, 403–408.
[8] McKhann, G., Drachman, D., Folstein, M., Katzman, R. *et al.*, *Neurology* 1984, *34*, 939–944.
[9] Wisniewski, H. M., Wegiel, J., Kolula, L., *Neuropathol. Appl. Neurobiol.* 1996, *22*, 3–11.
[10] Thal, D. R., Rüb, U., Schultz, C., Sassin, I. *et al.*, *J. Neuropath. Exp. Neurol.* 2000, *59*, 733–748.
[11] Griffin, W. S. T., Sheng, J. G., Mrak, R. E., in: Wasco, W., Tanzi, R. E. (Eds.), *Molecular Mechanisms of Dementia*, Humana Press, Totowa NJ, USA 1997, pp. 169–176.
[12] Dickson, W. D., *J. Neuropath. Exp. Neurol.* 1997, *56*, 321–339.
[13] Pike, C. J., Cumming, B. J., Cotman, C. W., *Exp. Neurol.* 1995, *132*, 172–179.
[14] Cullen, K. M., *Neuroreport* 1997, *8*, 1961–1966.
[15] Kato, S., Gondo, T., Hoshii, Y., Takahashi, M. *et al.*, *Pathol. Int.* 1998, *48*, 332–340.
[16] Bignami, A., Dahl, D., *Neuropathol. Appl. Neurobiol.* 1976, *2*, 99–110.
[17] Lenz, G., Manozzo, L., Gottardo, S.Achaval, M. *et al.*, *Brain Res.* 1997, *764*, 188–196.
[18] Xu, K., Malouf, A. T., Messing, A., Silver, J., *Glia* 1999, *25*, 390–403.
[19] Laping, N. J., Teter, B., Nichols, N. R., Rozovsky, I., Finch, C. E., *Brain Pathol.* 1994, *1*, 259–275.
[20] Inagaki, M., Nakamura, Y., Takeda, M., Nishimura, T., Inagaki, N., *Brain Pathol.* 1994, *4*, 239–243.
[21] Doering, L. C., *Mol. Neurobiol.* 1994, *7*, 265–291.
[22] Lukás, Z., Dráber, P., Bucek, J., Dráberová, E. *et al.*, *Histochem. J.* 1989, *21*, 693–702.
[23] Buée-Scherrer, V., Condamines, O., Mourton-Gilles, C., Jakes, R. *et al.*, *Mol. Brain Res.* 1996, *39*, 79–88.
[24] Goedert, M., Jakes, R., Van Mechelen, E., *Neurosci. Lett.* 1995, *189*, 167–170.
[25] Viklicky, V., Dráber, P., Hasek, J., Bártek, J., *Cell Biol. Int. Rep.* 1982, *6*, 725–731.
[26] Dráber, P., Lagunowich, L. A., Dráberová, E., Viklicky, V., Damjanov, I., *Histochemistry* 1988, *89*, 485–492.
[27] Riederer, B. M., Guadano-Ferraz, A., Innocenti, G. M., *Dev. Brain Res.* 1990, *56*, 235–243.
[28] Hochstrasser, D. F., Merril, C. R., *Appl. Theor. Electrophor.* 1988, *1*, 35–40.
[29] Lenette, D. A., *Am. J. Clin. Pathol.* 1978, *69*, 647–648.
[30] Fujita, K., Yamauchi, M., Matsui, T., Titani, K. *et al.*, *Brain Res.* 1998, *785*, 31–40.
[31] Bigbee, J. M., Bigner, D. D., Pegram, C., Eng, L. F., *J. Neurochem.* 1983, *40*, 460–467.
[32] Sloane, J. A., Hollander, W., Rosene, D. L., Moss, M. B. *et al.*, *Brain Res.* 2000, *862*, 1–10.
[33] Ciesielski-Treska, J., Goetschy, J. F., Aunis, D., *Eur. J. Biochem.* 1984, *138*, 465–471.
[34] Wallin, A., Bleenow, K., Rosengren, L. E., *Dementia* 1996, *7*, 267–272.
[35] Ishida, K., Kaneko, K., Kubota, T., Itoh, Y. *et al.*, *J. Neurol. Sci.* 1997, *151*, 41–48.
[36] Probst, A., Ulrich, J., Heitz, Ph. U., *Acta NeuroPathol.* 1982, *57*, 75–79.
[37] Saatman, K. E., Graham, D. I., McIntosh, T. K., *J. Neurotrauma* 1998, *15*, 1047–1058.
[38] Li, R., Fujitani, N., Jia, J. T., Kimura, H., *Am. J. Forensic. Med. Path.* 1998, *19*, 129–136.
[39] Holmberg, B., Rosengren, L., Karlsson, J. E., Johnels, B., *Movement Dis.* 1998, *13*, 70–77.
[40] Probst, A., Langui, D., Ulrich, J., *Brain Pathol.* 1991, *1*, 229–239.
[41] Su, J. H., Cummings, B. J., Cotman, C. W., *Acta Neuropathol.* 1998, *96*, 463–471.